

Electronic Structure of Sm and Eu Chalcogenides

A. Svane^{*1}, G. Santi¹, Z. Szotek², W. M. Temmerman², P. Strange³, M. Horne³, G. Vaitheeswaran⁴, V. Kanchana⁴, L. Petit⁵, and H. Winter⁶

¹ Department of Physics and Astronomy, University of Aarhus, DK-8000 Aarhus C, Denmark

² Daresbury Laboratory, Daresbury, Warrington WA4 4AD, United Kingdom

³ Department of Physics, Keele University, ST5 5DY, United Kingdom

⁴ Max-Planck-Institut für Festkörperforschung, D-70569 Stuttgart, Germany

⁵ Computer Science and Mathematics Division, and Center for Computational Sciences, Oak Ridge National Laboratory, Oak Ridge, TN 37831, USA

⁶ INFP, Forschungszentrum Karlsruhe GmbH, Postfach 3640, D-76021 Karlsruhe, Germany

Key words Valence transitions, rare earth semiconductors, gap, pressure coefficients

PACS 71.20.Eh, 71.28.+d, 71.15.Mb, 71.15.Nc

The ground state configuration of the monochalcogenides of Sm and Eu is determined from total energy calculations using the self-interaction corrected local-spin-density approximation. The Sm chalcogenides, with the exception of SmO, are characterized by divalent f^6 Sm ions, while all the Eu chalcogenides have divalent f^7 Eu ions in the ground state. With pressure, the Eu and Sm chalcogenides exhibit isostructural transitions into an intermediate valent state, which in the total energy calculations is represented by localized f^5 configurations on the Sm ions (f^6 on Eu ions) together with a partly occupied f -band at the Fermi level. The energy of the fundamental $f \rightarrow d$ transition, which determines the value of the semiconducting gap, is determined by total energy calculations of the charged rare earth ion (Eu^+ or Sm^+) in a supercell approach with one f -electron removed. The pressure coefficients are in excellent agreement with experiment, and the occurrence of isostructural transitions is intimately related to the closure of the band gap.

Copyright line will be provided by the publisher

1 Introduction

The valency of rare earth compounds continues to be a vivid research area [1, 2, 3, 4, 5, 6, 7, 8, 9, 10, 11, 12]. Of particular interest are systems where valency is influenced by controllable external parameters like pressure, temperature or alloying. The occurrence of isostructural phase transitions upon compression or anomalous pV -curves are distinct signatures of valence transformations. SmS is one of the most studied systems [1, 13, 14, 15]. At low temperature and zero pressure it crystallizes in the NaCl structure with a semiconducting behavior. At a moderate pressure of ~ 0.65 GPa SmS reverts to a metallic phase with a significant volume collapse of 13.5% [16], retaining however the NaCl structure. Photoemission experiments show distinctly different spectra for the two phases, which usually are interpreted on the basis of divalent f^6 ions in the ground state and mixed valent $f^5 - f^6$ ions in the high pressure metallic phase [17, 18]. Similar valence instabilities are observed in SmSe and SmTe [13, 17, 19, 2], which also crystallize in the NaCl structure. For these compounds the volume changes continuously, but anomalously, with pressure (at room temperature) [20, 2]. From the photoemission studies it is concluded that SmSe and SmTe at ambient pressure, like SmS, are also of predominantly f^6 character [17]. In the Eu chalcogenides, likewise having the NaCl structure at ambient conditions, the corresponding divalent f^7 configuration is relatively more stable, and the competing structural transition to the CsCl structure occurs before a valence transition, with the exception of EuO [21, 22]. Of particular interest is the reentrant behavior observed

* Corresponding author: e-mail: svane@phys.au.dk, Phone: +45 8942 3678, Fax: +45 8612 0740

in EuS [23], where reflectivity measurements revealed that EuS in the NaCl structure first undergoes an insulator-to-metal transition (around $P \sim 160$ kbar). Subsequently, at a pressure around $P \sim 200$ kbar, EuS transforms structurally to the CsCl structure, however at the same time becoming clearly insulating again. At even higher pressure, $P \sim 330$ kbar, metallic behavior sets in again. The equation of state shows a discontinuous volume jump at the structural transition, while the two insulator-to-metal transitions appear continuous.

The Sm and Eu chalcogenides (except SmO) are all semiconductors with a somewhat unusual gap structure, as the fundamental excitation is of f to d character [1]. This means that a localized f electron is excited into an itinerant conduction band, which is predominantly of rare earth d character.

The theoretical description of Sm and Eu compounds is a challenge due to the $4f$ -electrons. Conventional band structure calculations of SmS [24, 25, 26, 3], in the local density approximation (LDA) [27, 28], describe the f electrons as narrow bands, which leads to significant overestimation of the bonding of the f electrons [26]. To describe the localized nature of the f electrons more accurately, Schumann et al. [3] applied self-interaction corrections (SIC) to the six $4f_{5/2}$ states of SmS. This led to a semiconducting ground state. The gap, which is of charge transfer type (from $S-p$ to $Sm-d$ bands), was however too wide owing to the fact that the SIC scheme does not position the energy of the localized f states properly with respect to the band states. To remedy this, combinations of band theory and atomic model Hamiltonians have been discussed [4, 7, 12], in which the s , p , and d states are treated as band states within LDA, while the $4f$ states are treated as localized states including atomic multiplets. This procedure leads to good agreement between calculated spectral functions and measured photoemission and inverse photoemission spectra. Several adjustable parameters enter into this approach though, and these cannot easily be derived from first principles.

In the present work the above research issues will be pursued further. The trends of the electronic structures of the Sm [12] and Eu chalcogenides [11] will be reviewed. The zero temperature total energy of these compounds is calculated using the self-interaction corrected local-spin density (LSD) approximation [29]. The ground state valency of Sm and Eu is determined, and the behavior under hydrostatic compression is investigated. The semiconducting gaps and their pressure coefficients are calculated from total energy differences.

2 The SIC-LSD total energy method

The total energy functional of the LSD approximation is renowned for its chemical accuracy in describing conventional weakly correlated solids [28]. To facilitate an accurate description of the localized f electrons of rare earths, the self-interaction correction is included. This correction constitutes a negative energy contribution for an f -electron to localize, which then competes with the band formation energy gained by the f -electron if allowed to delocalize and hybridize with the available conduction states. Specifically, the SIC-LSD [29] total energy functional is obtained from the LSD as:

$$E^{SIC} = E^{LSD} - \sum_{\alpha}^{occ.} \delta_{\alpha}^{SIC} + E_{so}, \quad (1)$$

where α labels the occupied states and δ_{α}^{SIC} is the self-interaction correction for state α . As usual, E^{LSD} can be decomposed into a kinetic energy, T , a Hartree energy, U , the interaction energy with the atomic ions, V_{ext} , and the exchange and correlation energy, E_{xc} [27]. The self-interaction is defined as the sum of the Hartree interaction and the exchange-correlation energy for the charge density of state α :

$$\delta_{\alpha}^{SIC} = U[n_{\alpha}] + E_{xc}[n_{\alpha}]. \quad (2)$$

For itinerant states, δ_{α}^{SIC} vanishes identically, while for localized (atomic-like) states the self-interaction may be appreciable. In Sm and Eu compounds, it is of the order $\delta_{\alpha} \sim 80$ mRy per f -electron. The volume

dependence is rather weak reducing the overbinding of the LSD approximation for narrow band states. The last term in Eq. (1) is the spin-orbit energy:

$$E_{so} = \langle \xi(\vec{r}) \vec{l} \cdot \vec{s} \rangle. \quad (3)$$

We employ the atomic spheres approximation, whereby the crystal volume is divided into slightly overlapping atom-centered spheres of a total volume equal to the actual volume. In (3), the angular momentum operator, $\vec{l} = \vec{r} \times \vec{p}$, is defined inside each atomic sphere, with \vec{r} given as the position vector from the sphere center. Other relativistic effects are automatically included by solving the scalar-relativistic radial equation inside spheres.

The advantage of the SIC-LSD energy functional is that different valency scenarios can be explored by assuming atomic configurations with different total numbers of localized states. In particular, these different scenarios constitute local minima of the same functional, E^{SIC} in Eq. (1), and hence their total energies may be compared. The state with the lowest energy defines the ground state configuration. Note, that if no localized states are assumed, E^{SIC} coincides with the conventional LSD functional, i.e., the Kohn-Sham minimum of the E^{LSD} functional is also a local minimum of E^{SIC} . The interesting question is, whether competing minima with a finite number of localized states exist. This is usually the case in f -electron systems [5] and some 3d transition metal compounds [30], where the respective f and d orbitals are sufficiently confined in space to benefit appreciably from the SIC.

The SIC-LSD still considers the electronic structure of the solid to be built from individual one-electron states, but offers an alternative description to the Bloch picture, namely in terms of periodic arrays of localized atom-centered states (*i.e.*, the Heitler-London picture in terms of Wannier orbitals). Nevertheless, there still exist states which will never benefit from the SIC. These states retain their itinerant character of the Bloch form, and move in the effective LSD potential. The resulting many-electron wavefunction will consist of both localized and itinerant states. In contrast to the LSD Kohn-Sham equations, the SIC electron states, minimizing E^{SIC} , experience different effective potentials. This implies that to minimize E^{SIC} , it is necessary to explicitly ensure the orthonormality of the one-electron wavefunctions by introducing a Lagrangian multipliers matrix. Furthermore, the total energy is not anymore invariant with respect to a unitary transformation of the one-electron wavefunctions. Both of these aspects make the energy minimization more demanding to accomplish than in the LSD case. The electron wavefunctions are expanded in linear-muffin-tin-orbital (LMTO) basis functions [31], and the energy minimization problem becomes a non-linear optimization problem in the expansion coefficients. Further details of the present implementation can be found in Ref. [32].

The calculation of semiconductor gaps in the LDA has been a major issue for many years. The one-electron eigenvalues cannot be directly interpreted as physical excitation energies [33], and this is particularly so for the SIC-LSD eigenvalues of the localized states. In the present work, the gap is determined by total energy difference calculations, where the ground state (with localized f^n shells on the rare earth, $n = 6$ and $n = 7$ for Sm and Eu, respectively) is compared with an excited state realized in a supercell geometry with one rare earth atom in the ionized f^{n-1} configuration. The latter appears as a positively charged 'defect' in an otherwise perfect host, and the missing electron is artificially compensated by a uniform negative background charge density, in accord with the scheme often employed for charged impurities in semiconductors [34, 35]. In a real crystal this electron will be accommodated in some distant part of the crystal in an energy state given by the actual Fermi level, ϵ_F , and the energy of the excitation becomes:

$$E_{exc} = E^{SIC}(\text{Sm}^+) + \epsilon_F - E^{SIC}(\text{Sm}^0). \quad (4)$$

The fundamental gap is obtained when taking ϵ_F to coincide with the conduction band edge. The supercell employed in the present work contains four formula units.

3 Results and Discussion

3.1 Cohesive properties

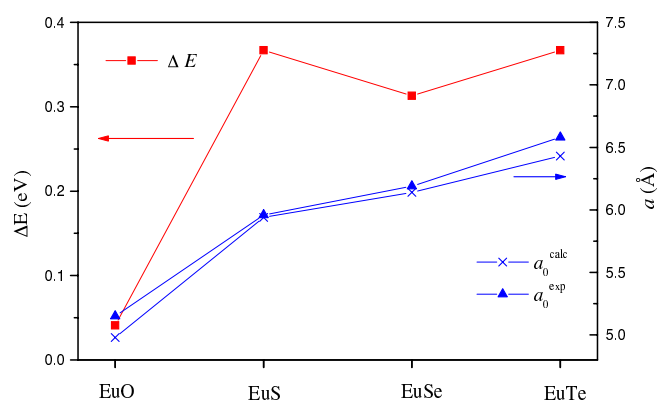


Fig. 1 Lattice constants (right axis) for the europium chalcogenides from experiment [36] (triangles) and SIC-LSD calculation (crosses). Also shown (left axis) is the calculated energy difference, $\Delta E = E(f^6) - E(f^7)$, between the trivalent and divalent Eu configurations (squares).

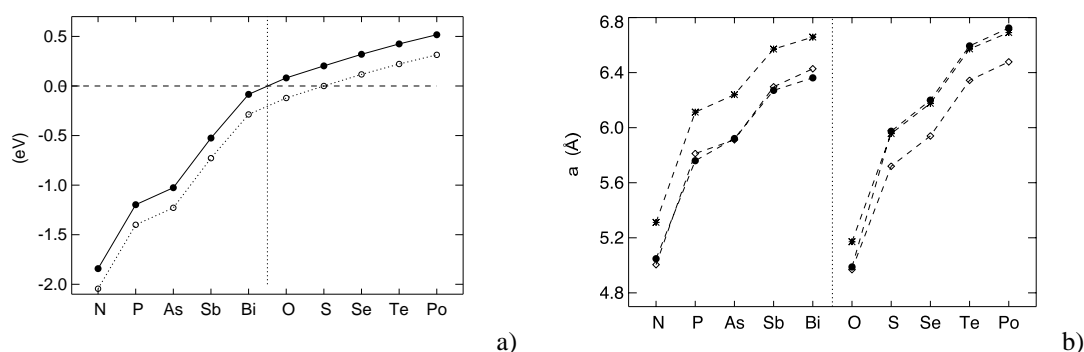


Fig. 2 a): Trivalent-divalent energy difference, $\Delta E = E(f^5) - E(f^6)$, of samarium compounds. The dashed line marks the calibrated curve [12]. b): Comparison of experimental [36] and theoretical lattice constants of SmX compounds. Experimental values are marked with solid circles, while lattice constants calculated assuming a divalent (trivalent) Sm ion are marked with stars (diamonds).

The figures 1 and 2 show the calculated lattice constants and valence stabilities for the Eu chalcogenides [11] and Sm pnictides and chalcogenides [12], respectively. Specifically, the total energy difference is calculated for the scenarios of trivalent and divalent rare earth ions (left axis of fig. 1 and full line in fig. 2 a)). A positive energy difference implies that the divalent configuration is preferred. This is the case in the Eu chalcogenides, in agreement with experiment. For the SmX compounds, the calculations reveal a strong preference of the f^5 configuration in the early pnictides, with the energy difference of 1.8 eV per formula unit in SmN. For the heavier Sm pnictides, the f^6 configuration becomes more and more advantageous, and for Bi it is only 0.08 eV higher than the trivalent configuration. Moving to the Sm chalcogenides, already in the Sm monoxide the f^6 configuration is found to be most favorable, by 0.08 eV, and in SmS by 0.20 eV. Hence, the SIC-LSD total energy predicts a valency transition of Sm between the Sm pnictides and the Sm chalcogenides. This is not in complete agreement with the experimental picture, according to

which the divalent and intermediate-valent states are almost degenerate in SmS, while SmO is trivalent and metallic [37, 38]. Thus, it appears that the SIC-LSD total energy functional overestimates the tendency to form the divalent configuration of Sm, by approximately 0.2 eV, in SmS. Assuming a similar error for all SmX compounds, this would imply that the calculated energy balance curve in fig. 2 a) should be lowered by approximately 0.2 eV. The dashed line of the figure shows the energy difference with such a correction. This switches the balance in favor of trivalency for SmO, in accord with experiments [37, 38]. A similar calibration was in fact already applied in fig. 1 [11], but in this case it does not affect the stability of the divalent ground state of Eu. The lattice constants are seen from fig. 1 (right axis) and fig. 2 b) to be in excellent agreement with experimental value for all compounds, corroborating the conclusion that a valency shift occurs between SmO and SmS.

For the Eu pnictides the relatively stable f^7 configuration changes the picture compared to the Sm pnictides [11]. Only EuN and EuP exist in the NaCl structure, and in these compounds Eu occurs as trivalent f^6 ions, in analogy to the SmN and SmP compounds. EuAs occurs in the Na₂O₂ structure, for which we find the divalent Eu configuration to be favored over the trivalent by 0.8 eV. EuSb does not exist at all. According to the SIC-LSD calculations, in hypothetical NaCl structure, EuSb would assume the divalent form (1.1 eV lower than the trivalent state), while EuAs would still be trivalent (0.2 eV lower than the divalent state).

In conclusion, the SIC-LSD total energy functional predicts correctly the trends in trivalent-divalent energy difference through the Eu and Sm pnictides and chalcogenides, but fails on a quantitative scale of the order of 0.2 eV. An error of this size is quite conceivable given that the functional does not contain any explicit contribution from the formation of atomic multiplets.

Table 1 Calculated isostructural transition pressures, P_t (in GPa), and volume changes (in %), of Eu and Sm monochalcogenides. Experimentally, the transition of SmS is discontinuous, while those of EuO, SmSe and SmTe (at room temperature) are continuous.

Compound	P_t (GPa)		Volume collapse (%)	
	Theory	Expt.	Theory	Expt.
EuO	19.3	30 ^a , 13 – 30 ^b	6.3	5 ^a
EuS	11.6	16 ^c	5.7	0 ^c
SmS	0.1	0.65 ^d , 1.24 ^e	11.1	13.5 ^d , 13.8 ^e
SmSe	3.3	~ 4 ^d , 3.4 ^e , 3 – 9 ^f , 2.6 – 4 ^g	9.8	8 ^d , 11 ^f , 7 ^g
SmTe	6.2	2 – 8 ^d , 5.2 ^e , 6 – 8 ^f , 4.6 – 7.5 ^g	8.4	9 ^f , 7 ^g

^a: Ref. [21]; ^b: Ref. [22]; ^c: Insulator-metal transition, Ref. [23]; ^d: Ref. [16]; ^e: Insulator-metal transition of Ref. [19]; ^f: Present author's estimates from figures of Ref. [2] and ^g: Ref. [39]. The volume changes for SmSe and SmTe are obtained by extrapolation over the transition range.

The trivalent phase of the chalcogenides becomes relevant at high pressure. In this phase the localised f^5 Sm ions or f^6 Eu ions coexist with a partly occupied narrow f -band, effectively describing an intermediate valent phase [12]. The calculated and measured transition pressures are listed in Table 1. The good agreement both for transition pressures and volume collapses proves that the bonding of the high pressure phase is well described in the SIC-LSD approximation, even if the true many-body wavefunction of the intermediate valence phase is much more complicated than the corresponding SIC-LSD wavefunction. This is in line with the general philosophy of the density functional approach of obtaining good total energy estimates from simple reference systems (non-interacting electrons). Note, that the transition pressures correspond to the total energy calibrated by the 0.2 eV correction discussed above. The present theory cannot describe the continuous nature of the transition observed for EuO, SmSe and SmTe. The

experiments were all conducted at room temperature. It would be interesting to investigate whether the continuous transition would exist at low temperature as well. For EuS the experiments show no anomalous compression curve [21], but the gap closes at 16 GPa, just before the structural transition to the CsCl structure (at 20 GPa) [23]. In a previous work we found the structural transition to occur at 13.7 GPa [6], however without an isostructural transition occurring first. Compared to that work, the present work has included the spin-orbit interaction. Due to the approximations involved, significant uncertainty persists, though, in the values of the total energy differences between different crystal structures.

3.2 Band gaps

The calculated band gap structures for EuS and SmS are shown in figure 3, namely the band edges and the localized f level, $\epsilon_f = E(f^{n-1}d) - E(f^n)$. The valence band maximum is the top of the full S p bands, while the conduction band minimum (CBM) is the lowest of the unfilled bands, which has primarily metal d character. The localized f level is calculated as outlined in section 2 from the total energy difference of supercells. Table 2 summarizes the results for the fundamental gap, which is the difference between the CBM and ϵ_f , as well as the pressure coefficient of the gap. The absolute value of the band gap is 0.6 eV too small for EuS and 0.6 eV too large for SmS, in comparison with the experimental values, while the calculated gaps of SmSe and SmTe are only marginally too large. Several uncertainties enter into the theory, most notably the general inadequacy of LDA band edges and the limited size of the supercell employed. A significant spin-splitting occurs at the bottom of the conduction band due to the presence of high-spin rare earth ions, which may render the Eu chalcogenides suitable for spin filtering [11]. The variation of the gaps with compression is in excellent agreement with the experimental pressure coefficients, which in all the cases considered reveal gaps decreasing at a rate around 100 meV/GPa. Only for SmTe the theory deviates significantly from experiment, with the theoretical pressure coefficient exceeding the experimental one by 45 %. The corresponding theoretical deformation potentials are $dE_{gap}/d \ln V = 4.18$ eV, 6.12 eV, 4.37 eV and 6.45 eV, for EuS, SmS, SmSe and SmTe, respectively.

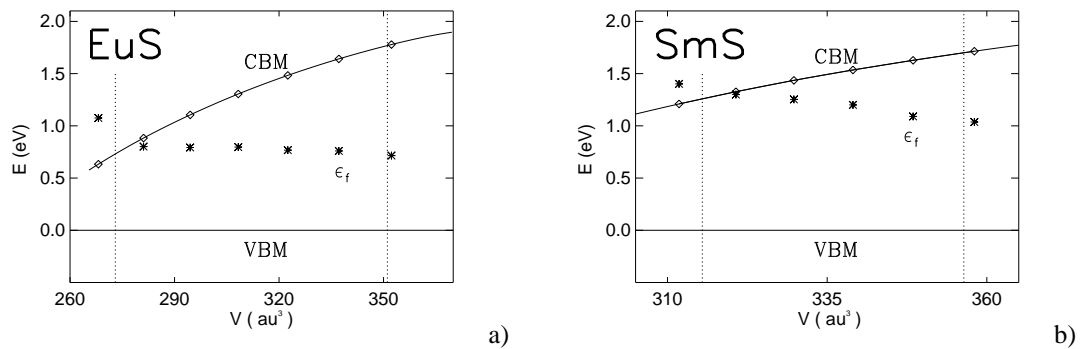


Fig. 3 Volume dependent gap structure of a): EuS and b): SmS. The conduction band minimum (CBM, squares) and localized f level, $\epsilon_f \equiv E(f^6d) - E(f^7)$ (stars) are shown relative to the valence band maximum (VBM). In a), the two vertical dotted lines mark the equilibrium zero pressure volume and the volume at $p = 20$ GPa, just before the transition to the CsCl structure. In b), the two vertical dotted lines mark the equilibrium zero pressure volumes of the $\text{Sm}(f^5)$ and $\text{Sm}(f^6)$ phases.

For EuS, we have in figure 3 a) marked the volume range covered during compression in the experimental works [21, 23] in the NaCl structure. One notices that the gap closes just prior to the NaCl \rightarrow CsCl structural transition, i. e. the insulator-metal transition occurs before the structural transition, in accord with the reflectivity measurements [23]. As discussed above, the present theory finds a discontinuous isostructural transition to occur in all the cases studied in Table 2, and in all cases the transition goes from

volumes where the system is still semiconducting to volumes lower than that where the gap closure occurs. Hence, the isostructural phase transitions coincide with insulator-metal transitions, both occurring as a consequence of the destabilization of the divalent f^n ion upon pressure. In figure 3 b) we have similarly marked the volumes (theoretical) of the two phases of SmS at zero pressure. In this case, since experiment also finds a discontinuous transition, the larger part of the volume range between the two marked volumes is in fact not accessible to experiment.

Table 2 Calculated bulk modulus, Energy gap, and pressure coefficient of gap, for EuS and Sm chalcogenides. All quantities are for the theoretical equilibrium configuration (Eu(f^7) and Sm(f^6) ions) and lattice constant of the NaCl structure.

Compound	Bulk modulus (GPa)		E_{gap} (eV)		$-dE_{gap}/dp$ (meV/GPa)	
	Present	Expt.	Present	Expt.	Present	Expt.
EuS	53.6	55(5) ^a	1.10	1.7 ^b	78	79 ^c , 110 ^b
SmS	53.4	42(3) ^d , 50.3 ^e , 47.6(5.0) ^f	0.71	0.15 ^a	115	100 ^c
SmSe	43.9	40(5) ^d	0.63	0.45 ^a	100	110 ^c
SmTe	37.6	40(5) ^d	0.70	0.65 ^a	172	119 ^c

^a: Ref. [1]; ^b: Ref. [23]; ^c: Ref. [21]; ^d: Ref. [16]; ^e: Ref. [40]; ^f: Ref. [41];

4 Summary

In this work, we have investigated the rare earth valency in the monpnictides and the monochalcogenides of Eu and Sm. In particular, we have focused on three of its manifestations, namely the cohesive properties, the pressure induced isostructural transitions and the semiconducting gap.

The cohesive properties of EuX and SmX compounds are well described by the local density approximation to density functional theory provided the self-interaction correction is applied to improve the description of the atomic-like f electrons. The bonding properties are quantitatively in agreement with experiment as evidenced by accurate lattice constants for both the trivalent pnictides and the divalent chalcogenides. Regarding the energy balance between the trivalent and divalent configurations of the rare earth in the studied solids, the SIC-LSD approach seems to underestimate the bonding in the trivalent configuration by ~ 0.2 eV, which can be considered a minor error. However, for an accurate description of the isostructural valence transitions induced by pressure it is a substantial inaccuracy. Correcting for this error we obtain good agreement with high pressure experimental results for EuO, EuS, SmS, SmSe and SmTe. The high pressure phase of the chalcogenides is described in the SIC-LSD one-electron picture as an array of f^{n-1} ions with an additional partially occupied f -band, leading to a total f occupation intermediate between $n - 1$ and n . For SmO, this is found to be the ground state. A small expansion of the SmO lattice, corresponding to an effective negative pressure, would lead to a transition to the divalent and semiconducting phase. This effect could be explored in SmO-SmS alloying experiments. The pressure variation of the semiconducting gap has been calculated from total energy differences, in all cases leading to decreasing gaps with pressure, and the isostructural transitions are intimately related to the closure of the gap.

Acknowledgements This work was partially funded by the EU Research Training Network (contract:HPRN-CT-2002-00295) ‘Ab-initio Computation of Electronic Properties of f-electron Materials’. Support from the Danish Center for Scientific Computing is acknowledged. The authors V.K. and G.V. acknowledge the Max-Planck Institute for financial support. The work of L.P. was supported in part by the Defense Advanced Research Project Agency and by the Division of Materials Science and Engineering, US Department of Energy, under Contract No. DE-AC05-00OR22725 with UT-Battelle LLC.

References

- [1] P. Wachter, *Handbook on the Physics and Chemistry of Rare Earths*, Vol. 19, chapter 132 (1994).
- [2] T. Le Bihan, S. Darracq, S. Heathman, U. Benedict, K. Mattenberger, O. Vogt, *J. Alloys. Comp.* **226**, 143 (1995).
- [3] R. Schumann, M. Richter, L. Steinbeck, and H. Eschrig, *Phys. Rev. B* **52**, 8801 (1995).
- [4] C. Lehner, M. Richter, and H. Eschrig, *Phys. Rev. B* **58**, 6807 (1998).
- [5] P. Strange, A. Svane, W. M. Temmerman, Z. Szotek, and H. Winter, *Nature* **399**, 756 (1999).
- [6] A. Svane, P. Strange, W. M. Temmerman, Z. Szotek, H. Winter, and L. Petit, *phys. stat. sol. (b)* **223**, 105 (2001).
- [7] V. N. Antonov, B. N. Harmon, A. N. Yaresko, *Phys. Rev. B* **66**, 165208 (2002).
- [8] A. Chainani, H. Kumigashira, T. Ito, T. Sato, T. Takahashi, T. Yokoya, T. Higuchi, T. Takeuchi, S. Shin, and N. K. Sato, *Phys. Rev. B* **65**, 155201 (2002); T. Ito, A. Chainani, H. Kumigashira, T. Takahashi, and N. K. Sato, *ibid.*, 155202 (2002).
- [9] S. Raymond, J. P. Rueff, M. D'Astuto, D. Braithwaite, M. Krisch, and J. Flouquet, *Phys. Rev. B* **66**, 220301 (2002).
- [10] A. Barla, J. P. Sanchez, Y. Haga, G. Lapertot, B. P. Doyle, O. Leupold, R. Rüffer, M. M. Abd-Elmeguid, R. Lengsdorf and J. Flouquet, *Phys. Rev. Lett.* **92**, 66401 (2004); A. Barla, J. P. Sanchez, J. Derr, B. Salce, G. Lapertot, J. Flouquet, B. P. Doyle, O. Leupold, R. Rüffer, M. M. Abd-Elmeguid, and R. Lengsdorf, *cond-mat/0406166*.
- [11] M. Horne, P. Strange, W. M. Temmerman, Z. Szotek, A. Svane and H. Winter, *J. Phys. Condens. Matter* **16**, 5061 (2004).
- [12] A. Svane, V. Kanchana, G. Vaitheeswaran, G. Santi, W. M. Temmerman, Z. Szotek, P. Strange, and L. Petit, (*Phys. Rev. B*, submitted (2004)).
- [13] A. Jayaraman, V. Narayanamurthi, E. Bucher, and R. G. Maines, *Phys. Rev. Lett.* **25**, 1430 (1970).
- [14] C. M. Varma, *Rev. Mod. Phys.* **48**, 219 (1976).
- [15] C. M. Varma and V. Heine, *Phys. Rev. B* **11**, 4763 (1975).
- [16] U. Benedict and W. B. Holzapfel, in *Handbook on the Physics and Chemistry of Rare Earths*, Vol. 17, ed. by K. A. Gschneidner, L. Eyring, G. H. Lander, and G. R. Choppin, (North-Holland, Amsterdam 1993) Chapter 113.
- [17] M. Campagna, E. Bucher, G. K. Wertheim and L. D. Longinotti, *Phys. Rev. Lett.* **33**, 165 (1974).
- [18] S.-J. Oh, and J. W. Allen, *Phys. Rev. B* **29**, 589 (1984).
- [19] V. A. Sidorov, N. N. Stepanov, L. G. Khvostantsev, O. B. Tsiok, A. V. Golubkov, V. S. Oskotski, and I. A. Smirnov, *Semicond. Sci. Technol.* **4**, 286 (1989).
- [20] A. Chatterjee, A. K. Singh, and A. Jayaraman, *Phys. Rev. B* **6**, 2285 (1972).
- [21] A. Jayaraman, A. K. Singh, A. Chatterjee, and S. Usha Devi, *Phys. Rev. B* **9**, 2513 (1974).
- [22] H. G. Zimmer, K. Takemura, K. Syassen, and K. Fischer, *Phys. Rev. B* **29**, 2350 (1984).
- [23] K. Syassen, *Physica B* **139 & 140**, 277 (1986).
- [24] O. V. Farberovich, *Phys. Stat. Sol. (b)* **104**, 365 (1981).
- [25] P. Strange, *J. Phys. C* **17**, 4273 (1984).
- [26] Z. W. Lu, D. J. Singh, and H. Krakauer, *Phys. Rev. B* **37**, 10045 (1988).
- [27] P. Hohenberg and W. Kohn, *Phys. Rev.* **136**, B864 (1964); W. Kohn and L. J. Sham, *Phys. Rev. A* **140**, 1133 (1965).
- [28] R. O. Jones and O. Gunnarsson, *Rev. Mod. Phys.* **61**, 689 (1989).
- [29] J. P. Perdew and A. Zunger, *Phys. Rev. B* **23**, 5048 (1981).
- [30] A. Svane and O. Gunnarsson, *Phys. Rev. Lett.* **65**, 1148 (1990); Z. Szotek, W. M. Temmerman and H. Winter, *Phys. Rev. B* **47**, 4029 (1993).
- [31] O. K. Andersen, *Phys. Rev. B* **12**, 3060 (1975); O. K. Andersen and O. Jepsen, *Phys. Rev. Lett.* **53**, 2571 (1984).
- [32] W. M. Temmerman, A. Svane, Z. Szotek and H. Winter, in *Electronic Density Functional Theory: Recent Progress and New Directions*, Eds. J. F. Dobson, G. Vignale and M. P. Das (Plenum, NY 1998.), p. 327.
- [33] J. P. Perdew and M. Levy, *Phys. Rev. Lett.* **51**, 1884 (1983); L. J. Sham and M. Schlüter, *Phys. Rev. Lett.* **51**, 1888 (1983).
- [34] C. G. Van de Walle and J. Neugebauer, *J. Appl. Phys.* **95**, 3851 (2004).
- [35] U. Gerstmann, P. Deak, R. Rurali, B. Aradi, Th. Frauenheim, and H. Overhof, *Physica B* **340**, 190 (2003).
- [36] P. Villars and L. D. Calvert, *Pearson's Handbook of Crystallographic Data for Intermetallic Phases*, 2. ed., (ASM International, Ohio, 1991).
- [37] J. M. Leger, P. Aimonino, J. Loriers, P. Dordor, and B. Coqblin, *Phys. Lett.* **80A**, 325 (1980).
- [38] G. Krill, M. F. Ravet, J. P. Kappler, L. Abadli, J. M. Leger, N. Yacoubi, and C. Loriers, *Solid State Commun.* **33**, 351 (1980).
- [39] O. B. Tsiok, V. A. Sidorov, V. V. Bredikhin, L. G. Khvostantsev, A. V. Golubkov, and I. A. Smirnov, *Solid State Commun.* **79**, 227 (1991).
- [40] Tu Hailing, G. A. Saunders, and H. Bach, *Phys. Rev. B* **29**, 1848 (1984).
- [41] E. Kaldis and P. Wachter, *Solid State Commun.* **11**, 907 (1972).